

# Neutron diffraction study of the magnetic structure of $\text{Na}_2\text{RuO}_4$

K.M. Mogare<sup>1</sup>, D.V. Sheptyakov<sup>2</sup>, R. Bircher<sup>3</sup>, H.-U. Güdel<sup>3</sup>, and M. Jansen<sup>1,a</sup>

<sup>1</sup> Max Planck Institute for Solid State Research, Stuttgart, Germany

<sup>2</sup> Laboratory for Neutron Scattering, ETH Zürich & Paul Scherrer Institute, 5232 Villigen PSI, Switzerland

<sup>3</sup> Department of Chemistry and Biochemistry, University of Bern, Bern, Switzerland

Received 12 April 2006

Published online 7 August 2006 – © EDP Sciences, Società Italiana di Fisica, Springer-Verlag 2006

**Abstract.** Nuclear and magnetic structures of sodium ruthenate (VI) have been studied by neutron powder diffraction in the temperature range 1.5–200 K.  $\text{Na}_2\text{RuO}_4$  crystallizes in the monoclinic structure, with space group  $P 2_1/c$ . The structure consists of apical corner sharing  $\text{RuO}_5$  trigonal bipyramids forming infinite chains running along the  $b$  axis. These infinite  $[\text{RuO}_3\text{O}_{2/2}]$  chains form a pseudo hexagonal close packing of rods with Ru–Ru distances of 3.51 Å within the chains and 5.30–5.47 Å between the chains. At  $T_N = 37.2$  K a magnetic transition leads to an antiferromagnetic state. The  $\text{Ru}^{6+}$  magnetic moments are ordered antiferromagnetically along the chains ( $b$ -axis), while the inter-chain interaction is ferromagnetic. A classical infinite chain model was fitted to the magnetic susceptibility data in order to estimate the strength of the nearest-neighbor exchange interactions along and between the chains, resulting in an intrachain coupling parameter of  $2J = -86$  K, and an interchain parameter  $J_\perp$  with  $|2J_\perp| = 3$  K.

**PACS.** 74.70.Pq Ruthenates – 75.25.+z Spin arrangements in magnetically ordered materials – 75.50.Ee Antiferromagnetics

## Introduction

Low dimensional oxides are widely studied due to their unusual physical properties. The term low dimensionality in this context usually refers to the short distances between metal atoms within a plane or along a chain, compared to the distances in other directions. The strongly directional character of these structure types induces high anisotropy of the exchange interactions, often giving rise to the peculiar charge or spin ordering phenomena [1]. Numerous low dimensional compounds are reported in the literature displaying various ferromagnetic and antiferromagnetic couplings within the chains [2–5]. In the system Na–Ru–O, several groups including us recently reported the unique crystal structure of a semiconducting oxide with pronounced one-dimensional character,  $\text{Na}_2\text{RuO}_4$  [6, 7]. The coordination of ruthenium in this oxide is exceptional as compared to the heavier alkali metal analogues,  $\text{A}_2\text{RuO}_4$  ( $\text{A} = \text{Cs}, \text{Rb}, \text{K}$ ) whose crystal structures contain the isolated tetrahedral oxoruthenate anions [8, 9]. In this family, the decrease in the size of the alkali metal cation leads to a more close packing of the ruthenium tetrahedra, thereby enhancing the magnetic interactions. Finally, the tetrahedral coordination of ruthenium is lost in the case of smaller sized sodium, in which the crystal structure is based on  $\text{RuO}_5$  trigonal bipyramids forming infinite  $-\text{Ru}-\text{O}-\text{Ru}-$  chains running along the  $b$ -axis.  $\text{Na}_2\text{RuO}_4$  orders anti-

ferromagnetically with a Néel temperature  $T_N \sim 37.2$  K. This antiferromagnetic transition, the unique coordination adopted by ruthenium in  $\text{Na}_2\text{RuO}_4$ , and the quasi trigonal arrangement of the magnetic centers which might cause magnetic frustration prompted us to investigate the low temperature magnetic properties. In this work, we report a low-temperature neutron diffraction study of the crystal and magnetic structures of  $\text{Na}_2\text{RuO}_4$ . We also correlate the magnetic structure obtained from neutron diffraction with the magnetic susceptibility data by fitting a classical infinite chain model to the experimentally measured magnetic susceptibility.

## Experimental

Polycrystalline samples of  $\text{Na}_2\text{RuO}_4$  were prepared in several batches from equimolar amounts of sodium peroxide and ruthenium dioxide in an oxygen stream at 898 K, as described in an earlier publication [6]. Each batch was checked with X-ray diffraction to confirm its purity as a single phase. A total amount of approximately 5 g was synthesized and sealed inside a 6 mm diameter vanadium container under argon for the neutron studies. Neutron powder diffraction experiments in the temperature range 1.5–200 K were carried out at the SINQ spallation neutron source of the Paul Scherrer Institute. The crystal structure parameters of  $\text{Na}_2\text{RuO}_4$  were refined from the powder patterns taken with the high-resolution diffractometer HRPT [10], operated in a High Intensity mode

<sup>a</sup> e-mail: M. Jansen@fkf.mpg.de

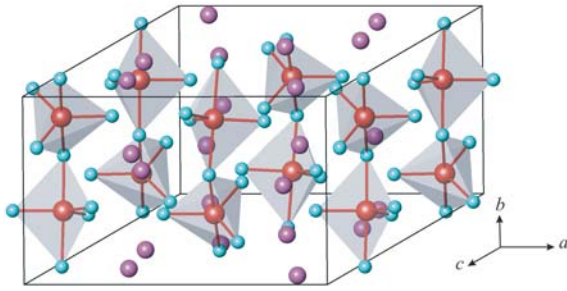


**Fig. 1.** Schematic view of the  $\text{Na}_2\text{RuO}_4$  crystal structure.  $\text{RuO}_5$  trigonal bipyramids sharing apical oxygen atoms form one-dimensional chains running along the  $b$ -axis.

with neutron wavelength  $\lambda = 1.886 \text{ \AA}$ . The data on magnetic ordering were obtained with the powder diffractometer DMC [11] located on a supermirror coated guide for cold neutrons at SINQ ( $\lambda = 4.20 \text{ \AA}$ ). The Fullprof [12] Suite of Programs was used for Rietveld refinements, and the Program SARAh [13] for symmetry analysis of the low-temperature magnetic structure.

## Results and discussion

### Crystal structure

The Rietveld refinements of the HRPT powder patterns yield the precise values of the structural parameters over a wide temperature range from 1.5 to 199 K. The results confirm the readily known model of the crystal structure of  $\text{Na}_2\text{RuO}_4$  (space group  $P 2_1/c$ ), which had been proposed based on a single crystal X-ray diffraction study at room temperature [7]. The compound does not undergo any structural phase transformation down to 1.5 K. The schematic view of the crystal structure of  $\text{Na}_2\text{RuO}_4$  is given in Figure 1 and a view of the Rietveld refinement plot of the HRPT data at 199 K is presented in Figure 2. The refined crystal structure parameters at two selected temperatures, 1.5 K and 199 K, at which the higher statistics acquisitions were done are listed in Table 1. The temperature dependence of the refined unit cell volume of  $\text{Na}_2\text{RuO}_4$  (see Fig. 3) shows a sudden decrease of the thermal expansion coefficient from more than  $5 \times 10^{-5} \text{ K}^{-1}$  above  $\sim 100 \text{ K}$  to less than  $6 \times 10^{-6} \text{ K}^{-1}$  below  $\sim 50 \text{ K}$ , i.e. it diminishes by about an order of magnitude. The interatomic bond length analysis shows that the Ru–O distances are almost constant over the whole investigated temperature range. Hence, the entire thermal expansion is due to the inter-polyhedral space, i.e. it is the surroundings of the Na ions which is being squeezed upon cooling down to 100 K and is then almost constant below  $\sim 50 \text{ K}$ .

### Magnetic ordering

Upon cooling the sample below  $T_N \sim 37.2 \text{ K}$ , the appearance of new reflexes in the neutron diffraction patterns (illustrated in Fig. 4) indicates the onset of long-range

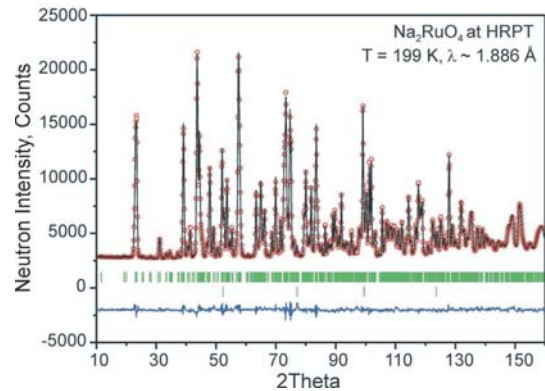


**Fig. 2.** Rietveld refinement plot of  $\text{Na}_2\text{RuO}_4$  powder neutron diffraction data from HRPT ( $\lambda = 1.886 \text{ \AA}$ ) at 199 K. The experimental points, calculated profile and the difference curve are shown. The two rows of ticks at the bottom indicate the calculated peak positions for the main phase and vanadium (the container material).

magnetic ordering of the  $\text{Ru}^{6+}$  ions. Figure 4 shows the diffraction patterns of  $\text{Na}_2\text{RuO}_4$  collected with the DMC diffractometer at two different temperatures:  $T = 39 \text{ K}$  (just above the magnetic transition temperature, lower curve) and  $T = 1.5 \text{ K}$  (saturated magnetic state). The total Bragg intensity at  $T = 39 \text{ K}$  is originating from nuclear scattering by the atoms of the chemical cell of  $\text{Na}_2\text{RuO}_4$ . The additional reflexes visible at  $T = 1.5 \text{ K}$  on the other hand are mainly of magnetic origin. Almost all the intensity of the  $(0\ 1\ 2)$  and  $(2\ 1\ 0)/(-2\ 1\ 2)$  peaks, as well as exactly the whole intensity of the  $(0\ 1\ 0)$  peak (since it is prohibited for the  $P 2_1/c$  space group of the crystal structure) arise from the neutron scattering on the long-range ordered lattice of magnetic  $\text{Ru}^{6+}$  ions. The  $hkl$ -indices (referring to the axes of the chemical unit cell) are indicated close to the magnetic diffraction peaks for clarity.

All additional lines originating from the neutron diffraction on the system of ordered  $\text{Ru}^{6+}$  magnetic moments can be indexed with integer indices within a parent unit cell of the crystal structure of  $\text{Na}_2\text{RuO}_4$ , though some of them are prohibited by its crystal symmetry. This implies the propagation vector of the magnetic structure  $\kappa = (0\ 0\ 0)$ . This propagation vector, together with the known crystal symmetry of the chemical cell ( $P 2_1/c$ ), and the positions of the two  $\text{Ru}^{6+}$  magnetic ions, serves as an input for the symmetry analysis of the possible magnetic ordering schemes. The representation analysis of the low-temperature magnetic structure was carried out with the Program SARAh [13]. All the predicted symmetry-allowed spin configurations have been checked with Rietveld refinements. Only two out of the three basis functions of a single irreducible representation ( $\psi_4$  and  $\psi_6$  of the irreducible representation  $\Gamma_2$  for both  $\text{Ru}^{6+}$  ions in the notation of SARAh) provide sets of calculated diffraction peaks consistent with our experimental data. Both basis functions correspond (as already expected from the appearance of additional lines in the patterns upon the magnetic transition) to the antiferromagnetic structures.

**Table 1.** Crystal structure parameters of Na<sub>2</sub>RuO<sub>4</sub> at  $T = 1.5$  K and  $T = 199$  K, refined from the HRPT powder neutron data, space group  $P 2_1/c$ . The thermal parameters for the atoms of each sort were constrained to equality in the refinements.

		$T = 1.5$ K	$T = 199$ K
$a$ , Å		10.65122 (8)	10.68366 (8)
$b$ , Å		7.01135 (4)	7.02334 (5)
$c$ , Å		10.82996 (8)	10.85282 (9)
$\beta$ , deg		119.1978 (4)	119.1884 (5)
Vol, Å <sup>3</sup>		706.013 (9)	710.936 (9)
Ru1 ( $x, y, z$ )	$x$	0.5004 (4)	0.5010 (4)
	$y$	0.2417 (4)	0.2431 (5)
	$z$	0.2511 (5)	0.2507 (5)
Ru2 ( $x, y, z$ )	$x$	-0.0002 (4)	-0.0008 (4)
	$y$	0.2294 (4)	0.2312 (4)
	$z$	0.2476 (5)	0.2481 (5)
$B(\text{Ru1, Ru2})$ , Å <sup>2</sup>		0.12 (3)	0.36 (3)
Na1 ( $x, y, z$ )	$x$	0.3008 (8)	0.3031 (10)
	$y$	0.4573 (9)	0.4610 (10)
	$z$	0.4104 (8)	0.4108 (10)
Na2 ( $x, y, z$ )	$x$	0.3505 (8)	0.3490 (9)
	$y$	0.5717 (9)	0.5646 (9)
	$z$	0.9153 (8)	0.9137 (9)
Na3 ( $x, y, z$ )	$x$	0.1893 (7)	0.1912 (9)
	$y$	0.5103 (13)	0.5143 (14)
	$z$	0.0885 (7)	0.0885 (9)
Na4 ( $x, y, z$ )	$x$	0.1520 (7)	0.1519 (8)
	$y$	0.0003 (11)	0.0022 (12)
	$z$	0.0993 (6)	0.0995 (8)
$B(\text{Na-Na4})$ , Å <sup>2</sup>		0.46 (4)	0.97 (5)
O1 ( $x, y, z$ )	$x$	0.1642 (4)	0.1626 (5)
	$y$	0.1422 (6)	0.1429 (6)
	$z$	0.3860 (4)	0.3861 (5)
O2 ( $x, y, z$ )	$x$	0.4818 (5)	0.4820 (5)
	$y$	0.6432 (6)	0.6473 (6)
	$z$	0.3904 (4)	0.3861 (5)
O3 ( $x, y, z$ )	$x$	0.3273 (5)	0.3296 (6)
	$y$	0.2502 (5)	0.2507 (5)
	$z$	0.2384 (5)	0.2401 (6)
O4 ( $x, y, z$ )	$x$	0.0069 (5)	0.0069 (5)
	$y$	0.3193 (7)	0.3204 (7)
	$z$	0.1001 (4)	0.0997 (5)
O5 ( $x, y, z$ )	$x$	0.1648 (4)	0.1656 (6)
	$y$	0.7234 (7)	0.7253 (5)
	$z$	0.2472 (6)	0.2485 (7)
O6 ( $x, y, z$ )	$x$	0.3420 (5)	0.3407 (5)
	$y$	0.6821 (7)	0.6812 (8)
	$z$	0.5953 (4)	0.5958 (4)
O7 ( $x, y, z$ )	$x$	0.4679 (4)	0.4677 (5)
	$y$	0.0108 (6)	0.0072 (6)
	$z$	0.6533 (4)	0.6538 (5)
O8 ( $x, y, z$ )	$x$	0.0484 (5)	0.0493 (5)
	$y$	0.4773 (5)	0.4784 (5)
	$z$	0.3512 (4)	0.3513 (5)
$B(\text{O1-O8})$ , Å <sup>2</sup>		0.22 (2)	0.56 (2)
$R_p$ , %		4.56	5.18
$R_{wp}$ , %		5.27	5.73
$\chi^2$		3.28	3.54

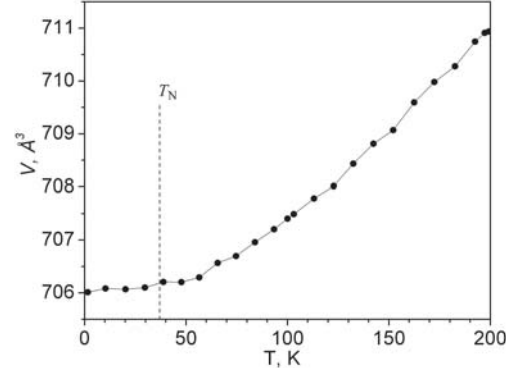


**Fig. 3.** Temperature dependence of the unit cell volume of the Na<sub>2</sub>RuO<sub>4</sub> crystal structure. The dashed line indicates the antiferromagnetic transition temperature.

In these two structures, the ferromagnetic layers of Ru<sup>6+</sup> ions are coupled antiferromagnetically along the chain direction. In other words, the coupling along the chains of RuO<sub>5</sub> trigonal bipyramids is antiferromagnetic, the chains being ferromagnetically coupled to each other in either of the  $a$ - $c$  in-plane directions. The magnetic structures described by the two basis functions  $\psi_4$  and  $\psi_6$  differ only in the direction of the magnetic moment with respect to the crystallographic axes of the chemical cell, pointing along  $a$  and  $c$ , respectively. Precise checking of these two possibilities has shown that the direction of magnetic moments is definitely not solely along  $c$ , since the intensity ratio between the (0 1 2) peak and the (2 1 0)/(-2 1 2) doublet does not perfectly match the experiment in this case. The agreement of calculation and experiment for magnetic moments aligned exactly along the  $a$  axis is good. However, with the available data quality it is not possible to exclude a certain mixing of these two directions. For this reason, the mixing was finally assumed for the refinements of the low temperature data. The refined components of magnetic moments along  $a$  and  $c$  stay roughly in the same proportion at all temperatures. The magnetic moment lies in the  $a$ - $c$  plane and is aligned predominantly along  $a$  with a weak  $c$ -component (at 1.5 K, the two components are refined to  $M_a = 1.85$  (2)  $\mu\text{B}$  and  $M_c = 0.56$  (7)  $\mu\text{B}$ ). An illustration of the determined magnetic structure model for Na<sub>2</sub>RuO<sub>4</sub> is shown in Figure 5.

It should be mentioned that the irreducible representation  $\Gamma_2$ , according to which the Na<sub>2</sub>RuO<sub>4</sub> compound orders magnetically, contains a third basis function,  $\psi_5$  in the notation of the program SARAh [13]. This function describes yet another scheme of the antiferromagnetic order, with the moments aligned along the  $b$  axis of the unit cell. Moreover, the symmetry does not restrict the magnitudes of the magnetic moments for the two Ru sites in our structure to be equal. From our experimental data, we estimate the effect of these two contributions on the magnetic moment of the Ru<sup>6+</sup> ions to be below 0.1  $\mu\text{B}$ , and they are therefore neglected in the analysis.

An additional difficulty in refining the exact values of the magnetic moments originates from the unknown magnetic form-factor of thermal neutron scattering for the

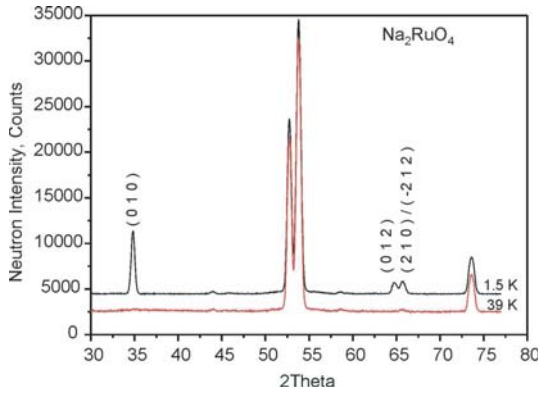


**Fig. 4.** Portions of the  $\text{Na}_2\text{RuO}_4$  neutron diffraction patterns taken with the DMC diffractometer at  $T = 39$  K (just above the magnetic transition, lower curve) and at  $T = 1.5$  K (saturated magnetic state, upper curve). The additional Bragg intensity at low temperature is due to the magnetic diffraction. The  $hkl$ -indices of the magnetic peaks refer to the axes of the chemical unit cell.

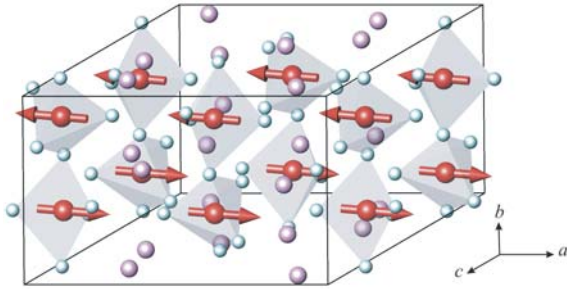


**Fig. 5.** Illustration of the magnetic structure of  $\text{Na}_2\text{RuO}_4$  at low temperature. The antiferromagnetically ordered chains of Ru ions are coupled ferromagnetically between each other. The magnetic Ru moments are aligned in the  $a$ - $c$  plane with the dominant  $a$ - and minor  $c$ -components.

$\text{Ru}^{6+}$  ions ( $4d^2$  electronic configuration). To the best of our knowledge, it has never been measured, or calculated to date. All modern Rietveld refinement codes use the approximations for the magnetic form-factors as tabulated in reference [14], and these only contain the form factors for Ru and  $\text{Ru}^+$  species, but not for the higher oxidation states of Ru. Obviously, these approximations cannot be used for  $\text{Ru}^{6+}$  ion, since its outer electronic shells are much more strongly localized. Indeed, if one tries the refinement with either of the two Ru or  $\text{Ru}^+$  form-factors, immediately an artificial unphysical “overall thermal parameter” for the magnetic phase has to be introduced in order to obtain the best fit quality. The exact determination of the  $\text{Ru}^{6+}$  form-factor is beyond the scope of the current investigation, thus in order to fit our data, the magnetic form-factors of various neighbouring  $4d$  elements in different oxidation states have been checked, and the best profile description (without necessity for any artificial overall thermal parameter for the magnetic phase) had been obtained with neutral Yttrium as a candidate. Hence, we have used the known and tabulated approximation for Y magnetic form-factor in our refinements.

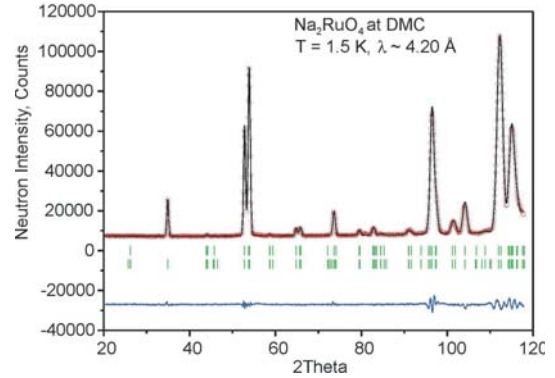


**Fig. 6.** Rietveld refinement of  $\text{Na}_2\text{RuO}_4$  powder neutron diffraction pattern obtained with the DMC diffractometer ( $\lambda = 4.20$  Å) at 1.5 K. The experimental points, calculated profile and the difference curve are shown. The two rows of ticks at the bottom indicate the calculated peak positions for the chemical and magnetic structures of  $\text{Na}_2\text{RuO}_4$ .

Not knowing the exact form-factor of the  $\text{Ru}^{6+}$  ion and substituting it by that of neutral Yttrium obviously introduces a certain systematic error into the absolute values of the refined magnetic moments. In order to estimate the possible uncertainty in the determination of the absolute value of the  $\text{Ru}^{6+}$  magnetic moment, it is worth comparing the refined values for different trial magnetic ions. They range from  $\sim 1.27 \mu\text{B}$  for  $\text{Ru}^+$  (with poor refinement quality) through  $1.53 \mu\text{B}$  for  $\text{Zr}^+$  to  $\sim 1.66 \mu\text{B}$  for the case of Y with sufficiently good refinement quality. We thus believe that the uncertainties in the absolute value of the magnetic moment determination in our case do not exceed  $\sim 10\%$ . More importantly these deviations, if any, are of a systematic character. If we would have known the magnetic form-factor of  $\text{Ru}^{6+}$ , then all the “true” values would differ from the ones derived in our study by a constant factor of not more than  $\pm 10\%$ .

An example of the DMC powder diffraction pattern refinement is shown in Figure 6. From the DMC powder data refinements at various temperatures, the temperature dependence of the ordered magnetic  $\text{Ru}^{6+}$  moment magnitude has been derived; it is presented in Figure 7. In order to estimate the antiferromagnetic transition temperature, the data of  $M_{\text{Ru}}(T)$  shown in Figure 7 were fitted to an empirical formula:

$$M(T) = M_0 [1 - (T/T_N)^\alpha]^\beta \quad (1)$$

with four free parameters:  $M_0$  — the saturated magnetic moment at  $T = 0$ ,  $T_N$  — the Néel temperature,  $\alpha$  and  $\beta$  — the refineable exponential parameters. The fit (solid curve in Fig. 7), has yielded the following parameters: the saturated low-temperature  $\text{Ru}^{6+}$  magnetic moment magnitude  $M_0 = 1.656 \pm 0.003 \mu\text{B}$ , antiferromagnetic transition temperature  $T_N = 37.22 \pm 0.06$  K, the exponents  $\alpha = 5.4 \pm 0.2$ , and  $\beta = 0.364 \pm 0.018$ .

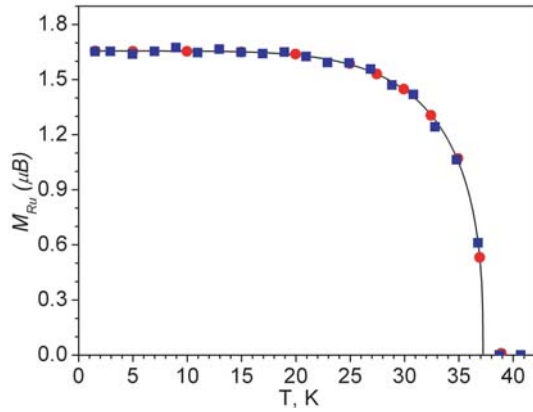


**Fig. 7.** Temperature dependence of the ordered Ru<sup>6+</sup> magnetic moment magnitude in Na<sub>2</sub>RuO<sub>4</sub>. Squares and circles correspond to the results of two independent measurement campaigns, carried out with a time interval of a few months. Except for the last few points (above 36 K), the error bars are comparable to the symbol sizes and for that reason are not shown for clarity. The solid line is a fit of the  $M_{\text{Ru}}(T)$  data with a function of equation (1) in the text.

### Magnetic susceptibility data interpretation

A discontinuity of the heat capacity at 37 K reported earlier [6], is in excellent agreement with the antiferromagnetic transition temperature  $T_N = 37.22 \pm 0.06$  K determined in the present neutron diffraction study. The magnetization data from reference [7] are also indicating the antiferromagnetic transition in the same temperature range. A dominant antiferromagnetic exchange interaction is evident from the magnetic susceptibility data. The data from reference [7] are plotted as  $\chi$  versus  $T$  in Figure 8. The broad maximum is characteristic for an antiferromagnetically coupled chain system. In order to obtain an estimate of the nearest-neighbor exchange parameter along the chains, we fitted a classical infinite chain model [15] to the data above 50 K, resulting in the solid line in Figure 8.

$$\chi = \frac{Ng^2\mu_B^2 S(S+1)}{3kT} \times \frac{1+u}{1-u} \quad (2)$$

with,

$$u = \coth \left[ \frac{2JS(S+1)}{kT} \right] - \frac{kT}{2JS(S+1)}.$$

The obtained  $2J = -86$  K for  $g = 1.77$  is somewhat higher than the value of  $2J = -56$  K estimated from the maximum of the  $\chi$  versus  $T$  curve in Shikano et al. [6]. Small deviations of the fit can be attributed to the fact that the model used describes a classical spin chain while the spin of the magnetic ions in our system is  $S = 1$ . Taking into account the simplicity of the model the determined fit is of satisfactory quality. Similar to the attempts described in Shikano et al. our model fit fails to account for the observed steep decrease of  $\chi$  below 50 K. The deviation of this purely one dimensional model from the data is attributed to the exchange interaction between the

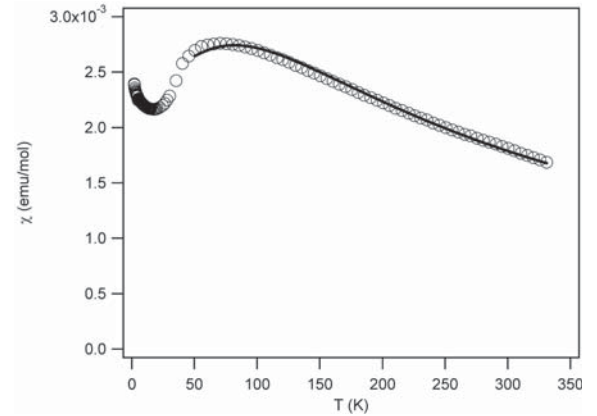


**Fig. 8.** Magnetic susceptibility of Na<sub>2</sub>RuO<sub>4</sub> measured in an applied field of 1 T (circles). The solid line represents a fit of the experimental data in the temperature range 50–330 K, calculated with a model for isolated chains of classical spins (Eq. (2)) with the parameters  $2J = -86$  K and  $g = 1.77$ .

chains, which eventually leads to the three dimensional antiferromagnetic ordering at  $\sim 37.2$  K. To obtain an estimate of the strength of the interchain coupling parameter  $|2J_{\perp}|$  we used  $T_N = 37.22$  K and the intrachain coupling  $2J = -86$  K. Within the mean-field approximation the three quantities are related by equation (3) [16].

$$|2J_{\perp}| = T_N / 1.28n [\ln(5.8 \cdot |2J| / T_N)]^{1/2} \quad (3)$$

with  $n = 6$  neighboring chains, according to the crystal structure, we get  $|2J_{\perp}| = 3$  K. The sign of the interaction parameter cannot be evaluated in this model; however the ferromagnetic coupling between the chains, as found in the present neutron diffraction study, determines it to be positive. The rise of  $\chi$  below 25 K must be due to paramagnetic impurities.

The ratio  $2J_{\perp}/2J = 3/86$  of inter- to intrachain exchange reflects the strong magnetic anisotropy of this material. The trigonal bipyramidal Ru coordination has approximate  $D_{3h}$  point symmetry. The axially elongated coordination results in singly occupied  $yz$  and  $zx$  orbitals. With an angle of approximately  $120^\circ$  between the  $z$  axes on adjacent Ru<sup>6+</sup> ions along the chain, there is enough overlap of the magnetic orbitals to produce the dominant antiferromagnetic intrachain coupling by a kinetic exchange mechanism.

### Conclusions

The present neutron diffraction study of Na<sub>2</sub>RuO<sub>4</sub> has confirmed the crystal structure determined by single crystal X-ray diffraction measurements. Trigonal bipyramids of RuO<sub>5</sub> form Ru-O-Ru chains along the  $b$  axis, these are packed in a hexagonal fashion. Below the magnetic ordering temperature of  $T_N = 37.22$  K the magnetic moments of the Ru<sup>6+</sup> ions are ordered antiferromagnetically along the chains, while the chains are coupled ferromagnetically between each other. The direction of magnetic moment of the

$\text{Ru}^{6+}$  ions is determined to be within the  $a$ - $c$  plane, with a dominant component along the crystallographic  $a$  axis, and possible minor component along the  $c$  axis. The low temperature saturated magnetic moment value amounts to  $1.66 \mu\text{B}$  under the assumption that the unknown magnetic form-factor of the  $\text{Ru}^{6+}$  ion may be sufficiently well approximated by that of a neutral Yttrium atom.

An estimate for the strength of the exchange interactions between the  $\text{Ru}^{6+}$  ions has been achieved by fitting a classical linear chain model to the experimental magnetic susceptibility data, yielding  $2J = -86 \text{ K}$  and  $|2J_{\perp}| = 3 \text{ K}$  for the intra- and interchain interactions, respectively.

Considering the trend observed in the magnetic interactions due to the smaller size of the alkali metal cation, it would be interesting to explore the lithium analogue of the title compound.

## References

1. T.N. Nguyen, P.A. Lee, H.-C. zur Loye, *Science* **271**, 489 (1996)
2. M. Hase, I. Terasaki, K. Uchinokura, *Phys. Rev. Lett.* **70**, 3651 (1993)
3. H. Fjellvag, E. Gulbrandsen, S. Aasland, A. Olsen, B. Hauback, *J. Solid State Chem.* **124**, 190 (1996)
4. H. Wu, M.W. Haverkort, Z. Hu, D.I. Khomskii, L.H. Tjeng, *Phys. Rev. Lett.* **95**, 186401 (2005)
5. K.E. Stitzer, W.H. Henley, J.B. Claridge, H.-C. zur Loye, R.C. Layland, *J. Solid State Chem.* **164**, 220 (2002)
6. M. Shikano, R.K. Kremer, M. Ahrens, H.-J. Koo, M.-H. Whangbo, J. Darriet, *Inorg. Chem.* **43**, 5 (2004)
7. K.M. Mogare, K. Friese, W. Klein, M. Jansen, *Z. Anorg. Allg. Chem.* **630**, 547 (2004)
8. D. Fischer, R. Hoppe, *Z. Anorg. Allg. Chem.* **591**, 87 (1990)
9. D. Fischer, R. Hoppe, K.M. Mogare, M. Jansen, *Z. Naturforsch.* **60b**, 1113 (2005)
10. P. Fischer, G. Frey, M. Koch, M. Könnecke, V. Pomjakushin, J. Schefer, R. Thut, N. Schlumpf, R. Bürge, U. Greuter, S. Bondt, E. Berruyer, *Physica B* **146** 276 (2000)
11. P. Fischer, L. Keller, J. Schefer, J. Kohlbrecher, *Neutron News* **11**, 19 (2000)
12. J. Rodríguez-Carvajal, *Physica B* **192**, 55 (1993)
13. A.S. Wills, *Physica B* **276–278**, 680 (2000)
14. *International Tables for Crystallography* (Kluwer Acad. Publications, 1992), Vol. C, p. **391**
15. O. Kahn, *Molecular Magnetism* (VCH Publishers, New York, 1993) p. 380
16. A.N. Vasiliev, O.L. Ignatchik, M. Isobe, Y. Ueda, *Phys. Rev. B* **70**, 132415 (2004)